Synthesis, Reactivity, and Dynamic Behavior of a Boron-Containing Silsesquioxane

Frank J. Feher,* Theodore A. Budzichowski,† and Joseph W. Ziller

Department of Chemistry, University of California, Irvine, California 92717

Received July 1, 1992

The reaction of $[(c\text{-}C_6H_{11})_7Si_7O_9(OH)_3]$ (**1**) with BI_3 affords $\{[(c\text{-}C_6H_{11})_7Si_7O_{12}B]_2\}$ (**2**), which has been characterized by multinuclear NMR spectroscopy and a single-crystal X-ray diffraction study. In the solid state, **2** adopts a structure containing trigonally planar boron atoms. Variable-temperature ^{13}C and ^{29}Si NMR spectra indicate that the same structure occurs in solution but that there is a low-energy intramolecular pathway for time-averaging all siloxy groups attached to boron. Compound **2** crystallizes in the orthorhombic space group $Pca2_1$ with a = 22.205 (4) Å, b = 23.992 (5) Å, c = 19.795 (8) Å, V = 10546 (5) Å, and Z = 4.

Introduction

Incompletely-condensed silsesquioxanes offer interesting possibilities as models for hydroxylated silica surfaces,[1] as ligands in homogeneous analogs of silica-supported catalysts,[2] and as "building blocks" for the systematic construction of structurally well-defined Si/O/M clusters.[3] The Si–O frameworks of silsesquioxanes are surprisingly flexible and capable of supporting a diverse range of molecular structures. Over the past several years we have been exploring the coordination chemistry of trisilanol **1**, which is readily available from the hydrolytic condensation of cyclohexyltrichlorosilane.[1a] In many cases, the complexes obtained from the reactions of **1** with either main group or transition metal halides are structurally similar to known tris(siloxide) or tris(alkoxide) complexes. In other instances, the unique coordination requirements of this tris-chelating ligand have profound effects on both the structure and reactivity of the expected product.[2a,b]

In order to identify coordination geometries that can be supported by trisilanol **1**, we have examined its reactions with a variety of trivalent transition-metal and main-group elements,[3a,4] where the inability of **1** to support trigonal planar coordination environments was expected to produce more complex structures. We have previously reported results concerning the reactions of **1** with trivalent complexes of aluminum,[2a] titanium,[4a] and vanadium.[4b] In this paper we describe the synthesis, characterization, reactivity, and dynamic behavior of an interesting boron-containing silsesquioxane dimer (**2**) prepared by the reaction of **1** with BI_3. The boron atoms in this complex adopt three-coordinate, trigonal planar arrangements to maximize π-bonding between boron and adjacent oxygen atoms, but variable-temperature NMR experiments suggest that species with higher coordination numbers are kinetically accessible.

Experimental Section

The general experimental protocol for the synthesis and purification of **1** appears elsewhere.[1a] BI_3 was obtained as a gift from Professor R. W. Taft (U. C. Irvine) and used without further purification. Except where noted, all operations were performed under nitrogen atmosphere either on a high-vacuum line with modified Schlenk techniques or in a Vacuum Atmospheres Corp. Dri-lab. All NMR spectra were recorded on a General Electric GN-500 (^1H, 500.1 MHz; ^{13}C, 125.03 MHz; ^{29}Si, 99.36 MHz) spectrometer. The CH_2 and CH resonances in the ^{13}C NMR spectra were assigned by using standard DEPT pulse sequences.

Synthesis of Borate Ester 2. One equivalent of solid BI_3 (1.03 g, 2.62 mmol) was added with vigorous stirring to a solution of **1** (2.55 g, 2.62 mmol) and triethylamine (2.0 g, 20 mmol) in benzene (70 mL) at 25 °C. The solution was stirred for 3 h, filtered to remove $[Et_3NH]I$, and then evaporated in vacuo (25 °C, 0.01 Torr) to afford an amorphous white foam. Extraction with warm toluene (~50 °C, ~50 mL), filtration through a pad of silica (to remove unreacted **1** and/or residual $[Et_3NH]I$), and cooling overnight to −34 °C afforded large colorless crystals, which were collected by vacuum filtration, washed with additional toluene (2 × 2.5 mL) and dried in vacuo (25 °C, 0.01 Torr). Yield: 1.11 g (43%). Concentration of the mother liquors to half of the original volume afforded an additional 0.74 g of **2** after 2 days at −34 °C. Total yield: 1.85 g (72%). For **2**, the characterization data are as follows. ^1H NMR (500.1 MHz, $CDCl_3$, 25 °C): δ 1.73 (br m, 35 H), 1.22 (br m, 35 H), 0.75 (br m, 7 H). $^{13}C\{^1H\}$ NMR (125.03 MHz, C_7D_8, 125 °C): δ 28.01, 27.89, 27.76, 27.50, 27.41, 27.34, 27.29 (s, for CH_2), 24.74, 24.44, 24.10 (s, 3:3:1 for CH). $^{13}C\{^1H\}$ (125.03 MHz, C_7D_8, −30 °C): δ 28.22, 28.09, 28.02, 27.95, 27.80, 27.75, 27.56, 27.44, 27.29, 27.24, 27.18, 26.93, 26.85 (s, for CH_2); 24.89, 24.23, 23.83, 23.65, 23.50 (s, 1:2:2:1:1 for CH). $^{29}Si\{^1H\}$ NMR (99.35 MHz, C_7D_8, 115 °C): δ −67.38, −68.16 (s, 1:6 relative ratio). $^{29}Si\{^1H\}$ (99.35 MHz, C_7D_8, −45 °C): δ −65.40, −66.16, −66.32, −67.62, −68.57 (s, 1:2:1:1:2). MS (70 eV, 200 °C; relative intensity): m/e no molecular ion observed, 898 ($M^+/2 - C_6H_{11}$, 100%), 815 ($M^+/2 - 2C_6H_{11}$, 10%). Anal. Calcd for $C_{84}H_{154}O_{24}B_2Si_{14}$ (found): C, 51.40 (51.33); H, 7.91 (7.71). MP: 365–380 °C dec. The ^{11}B NMR spectrum of **2** consists of a broad resonance (δ ~17 ppm, $v_{1/2}$ = 4000 Hz) which overlaps with the signal for ^{11}B present in the glass inserts of the probe.

Nonreactions of 2 with Lewis Bases. Recrystallized **2** (~200 mg, 0.10 mmol) and 0.02 mmol of a Lewis base (CH_3CN, Et_2O, THF, Me_3NO, Ph_3PO, Ph_3P, Et_3N, or $[R_4N^+]X$) were dissolved in $CDCl_3$ (~2.0 mL) in a 10-mm NMR tube and heated to 55 °C for 2 h. Examination of the NMR spectra (^1H, ^{13}C, ^{29}Si, and ^{31}P) revealed that no reactions had occurred; the resonances for **2** showed the same temperature dependence as in the absence of the Lewis bases.

Reaction of 2 with $Me_4SbOSiMe_3$. Solid **2** (0.300 g, 0.155 mmol) was added to a solution of $Me_4SbOSiMe_3$[5] (0.085 g, 0.313 mmol) in benzene (~5 mL) with stirring. After 12 h, the solvent was removed in vacuo

† T.A.B. is the recipient of a Fannie and John Hertz Foundation Predoctoral Fellowship.

(1) (a) Feher, F. J.; Newman, D. A.; Walzer, J. F. *J. Am. Chem. Soc.* **1989**, *111*, 1741–8. (b) Feher, F. J.; Newman, D. A. *J. Am. Chem. Soc.* **1990**, *112*, 1931–6. (c) Feher, F. J.; Budzichowski, T. A.; Blanski, R. L.; Weller, K. J.; Ziller, J. W. *Organometallics* **1991**, *10*, 2526–8. (d) Feher, F. J.; Budzichowski, T. A.; Rahimian, K.; Ziller, J. W. *J. Am. Chem. Soc.* **1992**, *114*, 3859–66.

(2) (a) Feher, F. J.; Blanski, R. L. *J. Am. Chem. Soc.* **1992**, *114*, 5886–7. (b) Feher, F. J.; Blanski, R. L. *J. Chem. Soc., Chem. Commun.* **1990**, 1614–6. (c) Feher, F. J.; Walzer, J. F.; Blanski, R. L. *J. Am. Chem. Soc.* **1991**, *113*, 3618–9. (d) Liu, J.-C.; Wilson, S. R.; Shapley, J. R.; Feher, F. J. *Inorg. Chem.* **1990**, *29*, 5138–9. (e) Feher, F. J.; Walzer, J. F. *Inorg. Chem.* **1991**, *30*, 1689–94. (f) Feher, F. J. *J. Am. Chem. Soc.* **1986**, *108*, 3850–2. (g) Budzichowski, T. A.; Chacon, S. T.; Chisholm, M. H.; Feher, F. J.; Streib, W. *J. Am. Chem. Soc.* **1991**, *113*, 689–91.

(3) (a) Feher, F. J.; Budzichowski, T. A.; Weller, K. J. *J. Am. Chem. Soc.* **1989**, *111*, 7288–9. (b) Feher, F. J.; Weller, K. J. *Organometallics* **1990**, *9*, 2638–40.

(4) (a) Feher, F. J.; Gonzales, S. L.; Ziller, J. W. *Inorg. Chem.* **1988**, *27*, 3440–2. (b) Feher, F. J.; Walzer, J. F. *Inorg. Chem.* **1990**, *29*, 1604–11.

(5) Schmidbaur, H.; Arnold, H. S.; Beinhofer, E. *Chem. Ber.* **1964**, *97*, 449–58.

0020-1669/92/1331-5100$03.00/0

Table I. Crystallographic Data for $[(c\text{-}C_6H_{11})_7Si_7O_{12}B]_2$ (2)

$C_{84}H_{154}B_2O_{24}Si_{14}$	fw = 1963
a = 22.205 (4) Å	space group = $Pca2_1$ (C_{2v}^5; No. 29)
b = 23.992 (5) Å	T = 183 K
c = 19.795 (8) Å	λ(Mo Kα) = 0.710 73 Å
V = 10546 (5) Å^3	μ = 0.0228 cm^{-1}
Z = 4	R_F = 10.6%[a]
ρ_{calcd} = 1.236 g/cm^3	R_{wF} = 10.3%[a]

[a] $R_F = 100[\sum||F_o| - |F_c||/\sum|F_o|]$ and $R_{wF} = 100\ [\sum w(|F_o| - |F_c|)^2/\sum w|F_o|^2]^{1/2}$ where $w^{-1} = \sigma^2(|F_o|) + 0.0007(|F_o|)^2$.

(25 °C, 0.01 Torr) to yield an amorphous white foam. The ^{1}H NMR spectrum revealed a new resonance for the $OSiMe_3$ group at ~0.200 ppm ($Me_4SbOSiMe_3$ = δ 0.232), but the ^{13}C NMR spectrum exhibited at least seven sharp resonances in the methine region (25.5–22.5 ppm) indicative of a mixture of products. Variable temperature NMR studies (7 to 80 °C) indicated that the apparent composition of the mixture was temperature dependent. All attempts to spectroscopically identify or isolate any of the components in the reaction mixture were unsuccessful.

X-ray Data Collection and Refinement for $[(c\text{-}C_6H_{11})_7Si_7O_{12}B]_2$ (2). Crystals of 2 suitable for X-ray diffraction were grown by allowing acetonitrile to slowly diffuse into a saturated C_6H_6 solution of 2 overnight. A colorless crystal measuring approximately 0.40 × 0.40 × 0.50 mm was mounted under a protective layer of Paratone-N (lube oil additive) on a glass fiber and aligned on a Siemens P3 automated four-circle diffractometer equipped with a locally modified Siemens LT-2 low-temperature device. Laue symmetry, crystal class, unit cell parameters, and the crystal's orientation matrix were determined at −90 °C by using techniques described by Churchill.[6] Intensity data were collected using the θ–2θ scan technique with Mo Kα radiation under the conditions given in Table I. All 8084 data were corrected for Lorentz and polarization effects and placed on an approximately absolute scale by means of a Wilson plot; no absorption correction was applied. The diffraction symmetry was *mmm*. On the basis of systematic absences (0*kl* *l* odd; *h*0*l*, *h* odd; *h*00, *h* odd; 00*l*, *l* odd), possible space groups were the noncentrosymmetric orthorhombic $Pca2_1$ (No. 29) or the centrosymmetric orthorhombic *Pcam* (alternate setting of *Pbcm*, No. 57). The former was chosen based on an analysis of intensity statistics provided by the program XPREP[7] and confirmed as the correct space group by successful solution and refinement of the structure.

All crystallographic calculations were performed using the SHELXTL-PLUS program set.[7] The analytical scattering factors for neutral atoms were used throughout the analysis;[8a] both the real ($\Delta f'$) and imaginary ($i\Delta f''$) components of anomalous dispersion[8b] were included. The quantity minimized during least-squares analysis was $\sum w(|F_o| - |F_c|)^2$ where $w^{-1} = \sigma^2(|F_o| + 0.0007(|F_o|)^2$.

The structure was solved by direct methods, which yielded one set of phase relationships with high internal consistency; a series of difference-Fourier syntheses revealed the positions of all non-hydrogen atoms. The carbon atoms of one cyclohexyl ring (C1–C6) were severely disordered and did not remain connected when refined at full occupancy. A second chair conformer (C2A–C6A) with overlap at C1 became apparent from a difference map after the first set of atoms were refined at half-occupancy, and both conformers were included in the final model. Refinement of the site occupancy factors for each ring resulted in convergence with C2–C6 at 52% occupancy and C2A–C6A at 48% occupancy. The interatomic distances for these rings are very inaccurate, suggesting that the disorder may be more severe, but the limited quantity and quality of the best diffraction data obtainable did not allow a more elaborate treatment of the problem.

Hydrogen atoms were included for nondisordered carbon atoms using a riding model with d(C–H) = 0.96 Å and U_{iso} = 0.08 Å^2.[9] Full-matrix least-squares refinement of positional and thermal parameters (anisotropic for B, O, Si) led to convergence with R_F = 10.6%, R_{wF} = 10.3%, and GOF = 2.06 for 717 variables refined against those 6117 data with $|F_o| > 2.0\sigma|F_o|$. It was not possible to determine the absolute configuration of the molecule: refinement of the Rogers η parameter[7] gave a value of 0 (2), and least-squares refinement of coordinates and thermal parameters for the enantiomer gave identical R_F, R_{wF}, and GOF. A final difference-Fourier synthesis showed several small peaks (0.85 e/Å^3) near the disordered cyclohexyl group.

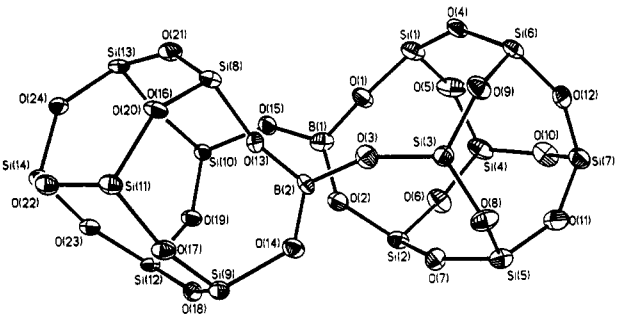

Figure 1. Perspective ORTEP plot of 2. For clarity, all carbon atoms have been omitted and thermal ellipsoids are shown at 20% probability. Selected interatomic distances (Å) and angles (deg) are as follows: B1–O1, 1.351 (23); B1–O2, 1.385 (22); B1–O15, 1.325 (23); B2–O3, 1.336 (19); B2–O13, 1.406 (18); B2–O14, 1.304 (20); Si1–O1, 1.609 (11); Si2–O2, 1.625 (12); Si3–O3, 1.587 (11); Si8–O13, 1.636 (12); Si9–O14, 1.671 (10); Si10–O15, 1.637 (11); O1–B1–O2, 120.2 (16); O1–B1–O15, 118.7 (15); O2–B1–O15, 121.1 (16); O3–B2–O13, 117.2 (14); O3–B3–O14, 122.9 (14); O13–B2–O14, 120.0 (13); B1–O1–Si1, 148.4 (13); B1–O2–Si2, 136.9 (11); B1–O15–Si10, 142.4 (11); B2–O3–Si3, 153.4 (11); B2–O13–Si8, 135.2 (10); B2–O14–Si9, 130.3 (10). Other Si–O distances vary from 1.590 to 1.650 Å. Other Si–O–Si and O–Si–O angles vary from 157.1 to 166.3 and 106.3 to 111.3°, respectively.

Table II. Exchange Rates Calculated From Simulated ^{13}C and ^{29}Si NMR Spectra

	k_{obs}, s^{-1}			k_{obs}, s^{-1}	
T, K	from ^{13}C	from ^{29}Si	T, K	from ^{13}C	from ^{29}Si
228		1.60	293	2.20 × 10^2	
243	5.00	5.00	303	3.60 × 10^2	3.00 × 10^2
253	1.28 × 10		313	5.00 × 10^2	
258		1.70 × 10	318		6.00 × 10^2
263	2.80 × 10		333	1.10 × 10^3	1.03 × 10^3
273	6.20 × 10	5.40 × 10	348	1.60 × 10^3	2.20 × 10^3
278			363	4.50 × 10^3	4.50 × 10^3
283	1.25 × 10^2	1.25 × 10^2	388		1.40 × 10^4
288		1.60 × 10^2	393	2.50 × 10^4	

Simulation of Variable-Temperature ^{13}C and ^{29}Si NMR Spectra. The NMR spectra for 2 were recorded on a GN-500 (^{13}C = 125.03 MHz, ^{29}Si = 99.35 MHz) spectrometer. The ^{13}C NMR spectra were obtained using a 30° pulse width and a 2-s delay between pulses. A total of 640 transients were obtained at each of the temperatures listed in Table II, and the resulting spectra were referenced to the quaternary carbon of C_7D_8 (137.5 ppm). The ^{29}Si NMR spectra were recorded using a 30° pulse width and a 10-s delay between pulses. Inverse-gated decoupling was used in order to minimize nuclear-Overhauser effects. A total of 540 transients were obtained at each of the temperatures listed in Table II for this nucleus, and the resulting spectra were referenced to an external sample of tetramethylsilane (50% in C_6D_6, 0.0 ppm). Under these conditions there appeared to be no appreciable effects due to differential relaxation; both the ^{13}C (methine region) and ^{29}Si NMR spectra gave reliable integrations for spectral simulations.

The thermocouple used in the variable temperature unit was calibrated by recording single-transient ^{1}H NMR spectra of neat methanol at a variety of temperatures according to ref 10. Since the observed and calculated temperatures were in excellent agreement (±0.5 °C), no corrections were applied.

The spectra were simulated using the expressions derived by Rogers and Woodbrey for uncoupled two-site exchange,[11] with programs written in BASIC for a Macintosh IIx computer.[12] The low-temperature ^{29}Si NMR spectrum and the methine (CH) region of the low-temperature ^{13}C NMR spectrum both exhibit five resonances with relative integrated intensities of 2:2:1:1:1. At higher temperatures, three resonances with relative integrated intensities of 3:3:1 are produced by time-averaging.

(6) Churchill, M. R.; Lashewycz, R. A.; Rotella, F. J. *Inorg. Chem.* **1977**, *16*, 265.
(7) Siemens (Nicolet) Instrument Corporation, Madison, WI, 1987.
(8) *International Tables for X-Ray Crystallography*; Kynoch Press: Birmingham, England, 1974; (a) pp 99–101; (b) pp 149–50.
(9) Corfield, P. W. R.; Doedens, R. J.; Ibers, J. A. *Inorg. Chem.* **1967**, *6*, 197.
(10) Sandstrom, J. *Dynamic NMR Spectroscopy*; Academic Press: New York, 1982.
(11) Rogers, M. T.; Woodbrey, J. C. *J. Chem. Phys.* **1959**, *30*, 899.
(12) A copy of the program is available from F.J.F. upon request.

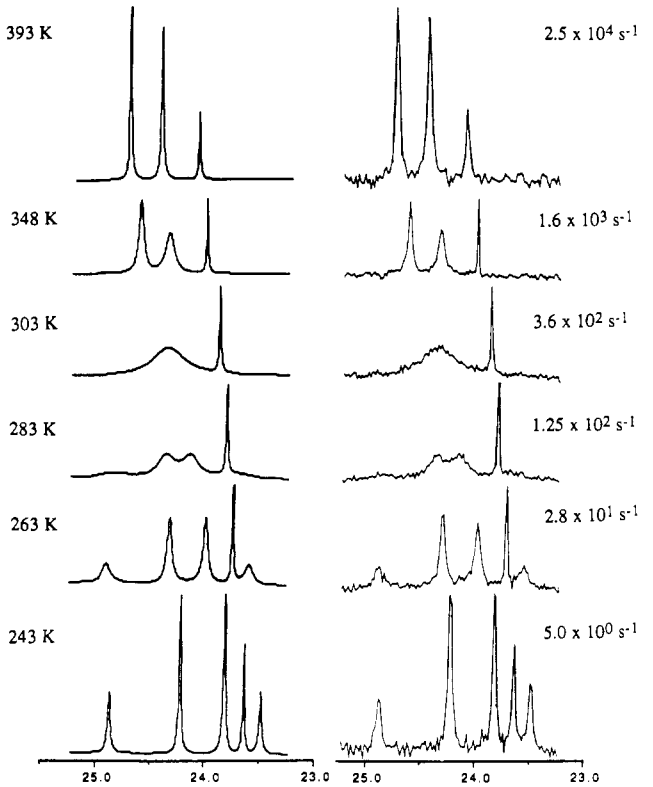

Figure 2. Simulated (left) and observed (right) ^{13}C NMR spectra of **2**. Temperatures are given on the left. Rate constants used for simulations are shown on the right.

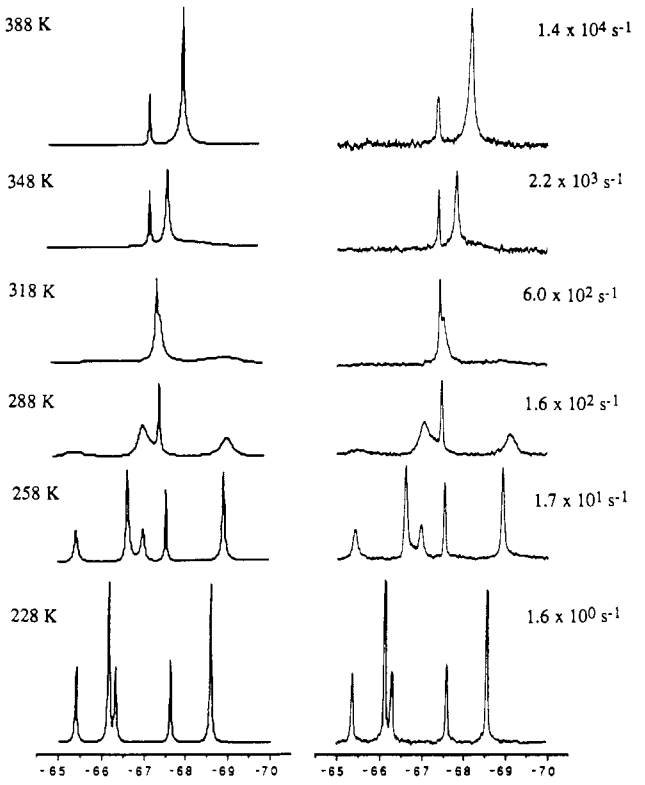

Figure 3. Simulated (left) and observed (right) ^{29}Si NMR spectra of **2**. Temperatures are given on the left. Rate constants used for simulations are shown on the right.

The spectra were numerically treated as the sum of three different sets of Lorentzian curves. Two of the sets, each consisting of two signals with a constant ratio (A:B) of 2:1, each coalesce at high temperature to produce one resonance with an integrated intensity corresponding to three Si nuclei. The third set consists of a single resonance (for one Si), which is unaffected by the exchange; this resonance is assigned to Si atoms which are furthest from the boron atom. The exchange process responsible for coalescence can be characterized by a single rate constant (k), which must be the same for all sites involved in the exchange process. For the two sets of resonances with ratios of 2:1 (A:B), the exchange process leading to coalescence can be described as an equilibrium:

$$A \underset{2k}{\overset{k}{\rightleftharpoons}} B$$

In each case values for T_2 (transverse relaxation time) were estimated from the average width at half-height, W_{0A}, of the unique (i.e., non-exchanging) resonance using eq 1.[10]

$$W_{0A} = (\pi T_2)^{-1} \quad (1)$$

Visual comparisons of the calculated and observed spectra were used to determine the best value for the rate constant, k (±10%), at each temperature (Table II). Selection of "the best" rate constant was relatively straightforward because changes in the rate constant have a dramatic effect on the calculated band shapes (Figures 2 and 3).

The five resonances in both the ^{13}C and ^{29}Si NMR spectra displayed temperature-dependent chemical shifts which required modeling in order to obtain satisfactory results during spectral simulation. Attempts to model this temperature dependence by simply extrapolating the temperature dependence observed prior to the onset of coalescence produced totally unsatisfactory results because it drastically overestimated the effects at high temperature. A more satisfactory model for the temperature dependence used the time-averaged chemical shifts observed at the fast-exchange limit to calculate chemical shifts for the peaks contributing to the observed resonance. (The observed chemical shift is the weighted-average.) Linear functions (i.e., $\delta = \delta_0 + \alpha T$) produced good simulated spectra at both the high-temperature and low-temperature limits, but they did not produce satisfactory simulations at intermediate temperatures. Excellent simulations were obtained by introducing a second-order term to describe the temperature dependence and fitting the observed temperature dependence with a second-order polynomial: $\delta = \delta_0 + \alpha T + \beta T^2$. The chemical shifts and coefficients used with this model are provided in the supplementary material.

Results and Discussion

Synthesis and X-ray Crystal Structure of 2. The reaction of equimolar amounts of BI_3 (an easily weighed solid) with trisilanol **1** in benzene/Et_3N resulted in the immediate formation of triethylammonium iodide, which was easily removed by vacuum filtration. The room-temperature ^{13}C and ^{29}Si NMR spectra of the crude product obtained after evaporation of the solvent (25 °C, 0.01 Torr) exhibited a complex pattern of broad resonances. Recrystallization from benzene/acetonitrile afforded a high yield of beautiful multifaceted crystals, but the ^{13}C and ^{29}Si NMR spectra of these crystals exhibited the same poorly-resolved pattern of broad resonances. The identity of this crystalline compound was eventually established as boron dimer **2** on the basis of a single-crystal X-ray diffraction study on one of the many well-formed crystals. An ORTEP plot of this dimer is shown in Figure 1.

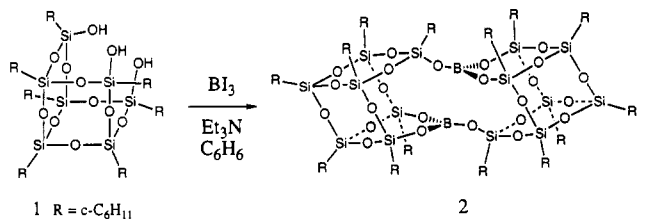

1 R = c-C_6H_{11} 2

The relatively high R-factor for the structure (current R_F = 10.6%, R_{wF} = 10.3%) prevents a serious discussion of bond distances and angles, but it is clear from Figure 1 that the two boron atoms adopt trigonal planar geometries. This is the first heterosilsesquioxane derived from trisilanol **1** to contain trigonal planar heteroatoms, but the general bonding scheme with respect to the silsesquioxane framework has been observed before in two structurally related complexes (i.e., **3** and **4**).[2e,g]

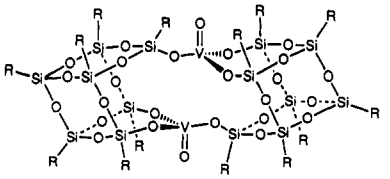

3

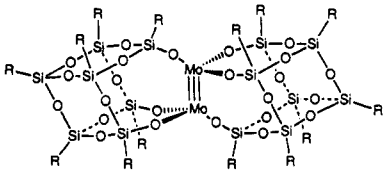

4

NMR Characterization of 2. The high yield of **2** obtained after recrystallization suggested that the poorly-resolved NMR spectra for this compound were not due to the presence of many products but were instead the result of a fluxional process which produced coalescence behavior near room temperature. This was confirmed by variable-temperature ^{13}C and ^{29}Si NMR studies.

At low temperature (≤ -30 °C) both the ^{29}Si NMR spectrum and methine (*C*H) region of the ^{13}C NMR spectrum exhibit five resonances with relative integrated intensities of 2:2:1:1:1, indicative of C_s molecular symmetry for the ligand and an exchange process which is slow relative to the ^{13}C and ^{29}Si NMR time scales. At 110 °C the exchange process which equilibrates the structure is much more rapid than the NMR time scales. The ^{13}C NMR spectrum exhibits three resonances with relative intensities of 3:3:1, consistent with a time-averaged C_{3v}-symmetric structure. The high-temperature ^{29}Si NMR spectrum only exhibits two resonances, but the 6:1 ratio of integrated intensities is also consistent with a time-averaged C_{3v}-symmetric structure; the resonance attributable to six Si nuclei is obviously a superposition of two resonances with integrated intensities of 3:3. At room temperature the rate of exchange is comparable to $1/T_2$ for both ^{29}Si and ^{13}C, and the spectra are broad and quite complex due to the onset of coalescence phenomena.

The rates of exchange at a number of different temperatures were empirically estimated by using an dynamic line shape analysis program;[12] calculated and experimentally observed ^{13}C and ^{29}Si spectra are shown in Figures 2 and 3. Eyring plots of the temperature-dependent exchange rates obtained from dynamic line shape analysis are illustrated in Figure 4.

Because the same exchange process is responsible for coalescence phenomena in both the ^{29}Si and the ^{13}C NMR spectra, the activation parameters derived from both plots in Figure 4 should be equal. This is indeed the case: ΔH^* and ΔS^* calculated from a "least-squares" fit of the ^{13}C NMR data (9.1 ± 0.3 kcal/mol and −17 ± 2 eu, respectively) are equal within experimental limit of uncertainty to ΔH^* and ΔS^* calculated from the ^{29}Si NMR data (9.2 ± 0.2 kcal/mol and −17 ± 1 eu). The small ΔH^* is a reflection of the relative ease with which the exchange process occurs, while the relatively large negative ΔS^* is consistent with an exchange mechanism with a highly ordered transition state or intermediate.[13]

It was not possible to unambiguously identify the sequence of steps responsible for producing the high-temperature, time-averaged ^{13}C and ^{29}Si NMR spectra. Nevertheless, a number of observations support the mechanism proposed in Scheme I: (1) the crystal structure determination establishes **2** as the ground state; (2) the propensity of borate esters to accept a fourth ligand and the close proximity of O13 and O2 to nearby boron atoms makes oxygen-bridged species likely intermediates in the exchange process; (3) complex **5**, although not directly observed in this system, possesses the same siloxy-bridged structure observed previously in stable trivalent dimers containing Al,[3a] Ti,[4a] and V[4b] instead of B; (4) the large negative ΔS^* (−17 eu) is consistent with an intermediate possessing higher coordination at boron and fewer degrees of freedom; (5) although difficult to rule out entirely, catalysis by trace impurities (e.g., H_2O) is unlikely because the NMR spectra are reproducible regardless of the source of both the sample and deuterated solvent. (Added water eventually hydrolyzes **2**, but it does not effect the rate of the exchange process.)

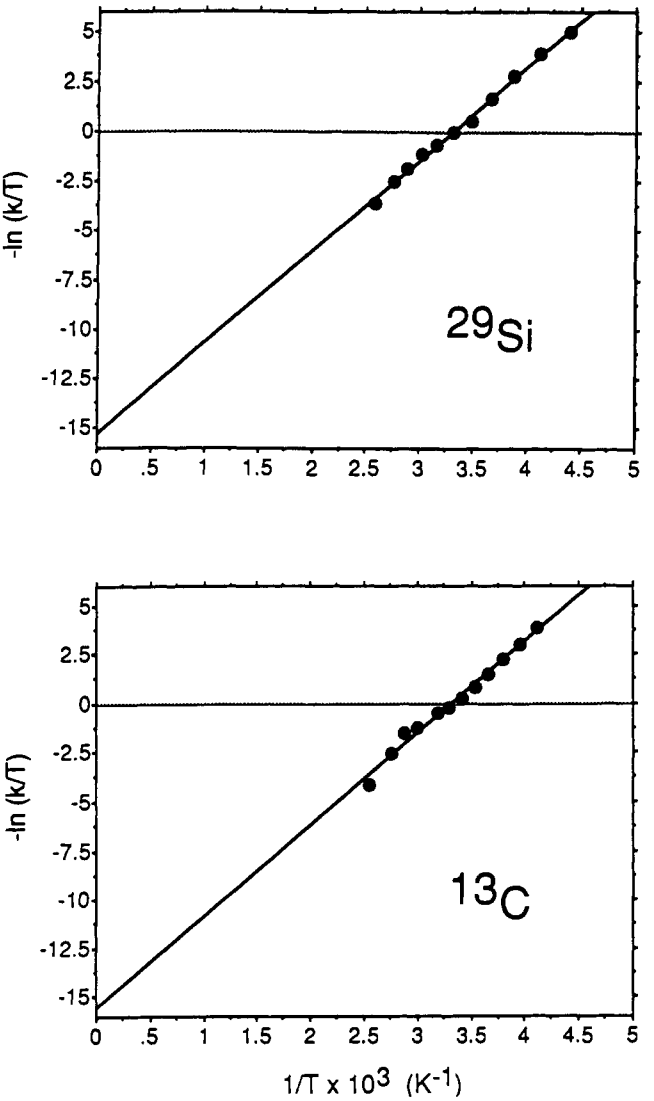

Figure 4. Eyring plots of temperature-dependent exchange rates derived from dynamic line shape analysis. Top: Activation parameters from ^{29}Si data. $\Delta H^* = 9.2 \pm 0.2$ kcal/mol, and $\Delta S^* = -17 \pm 1$ eu. Bottom: Activation parameters from ^{13}C data. $\Delta H^* = 9.1 \pm 0.3$ kcal/mol, and $\Delta S^* = -17 \pm 2$ eu.

The most likely alternative to the mechanism proposed in Scheme I, which would effect coalescence by producing small amounts of monomer **6**, is illustrated in Scheme II. As attractive as it might appear to be, this mechanism can be easily ruled out because the coalescence behavior is independent of concentration; all equilibrating species must have the same molecularity with respect to boron (i.e., all are monomers, all are dimers, etc.).

Reactivity of 2 toward Lewis Bases. The apparent ability of boron atoms in **2** to achieve four-coordination by transiently forming **5** suggested that it might be possible to prepare stable Lewis adducts of **2** (e.g., **7**). It also suggested that monomeric adducts (e.g., **8**) formally derived from the coordination of the Lewis base to **6** would be accessible. Unfortunately, all attempts

(13) Jackman, L. M. *Dynamic Nuclear Magnetic Resonance Spectroscopy*, Academic Press: New York, 1975; and references therein.

Scheme I

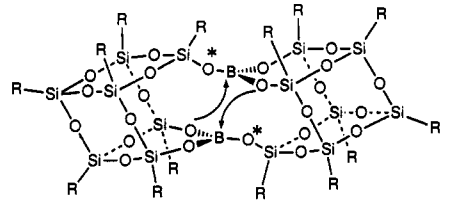

2

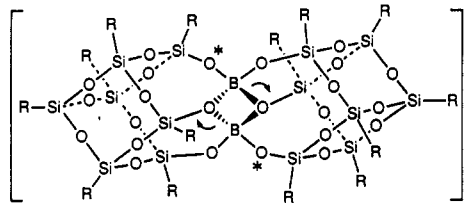

5

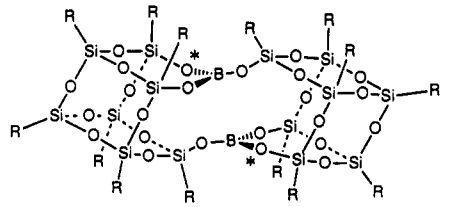

2'

Scheme II

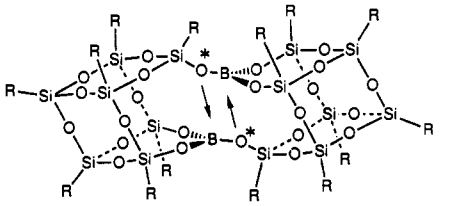

2

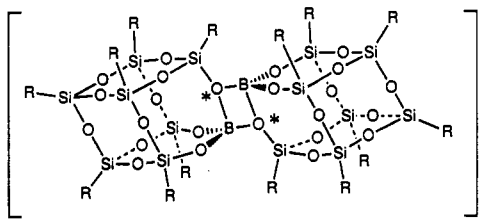

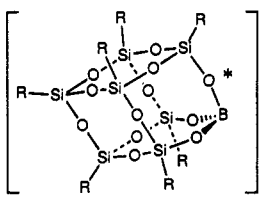

6

to prepare stable, four-coordinate Lewis adducts were unsuccessful. Despite the apparent presence of a vacant acceptor orbital on boron, Lewis bases such as Et_2O, THF, Me_3NO, Ph_3PO, Ph_3P, Et_3N, and halides (as $[R_4N^+]$ salts) are unreactive toward **2**. Even CH_3CN, which has minimal steric requirements, exhibits no detectable reactivity toward **2**. We can only speculate about reasons for the apparent inertness of **2** toward these potential Lewis bases, but molecular models strongly suggest that steric effects are probably *not* the dominant force. Dimer **2**—with trigonal BO_3 moieties—simply appears to be much more stable than a pyramidal Lewis base adduct.

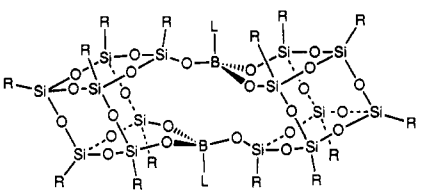

7

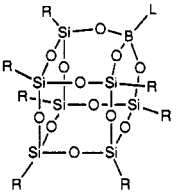

8

Stronger nucleophiles, such as alkali-metal alkoxides and siloxides, appear to promote skeletal rearrangements of the silsesquioxane framework, rather that coordinate to boron. Only the mild siloxide donor $Me_4SbOSiMe_3$,[5] which has been used in other cases[3] to prepare stable Lewis adducts without compromising the integrity of silsesquioxane frameworks, appears to react cleanly with **2**. Unfortunately, the product from this reaction appears to be both labile and conformational labile. All attempts to isolate a stable adduct from this mixture or characterize the reaction product(s) by NMR spectroscopy were unsuccessful.

Concluding Remarks

A recurring theme in the chemistry of metallasilsesquioxanes is the ability of silsesquioxane frameworks to accommodate the contortions necessary for otherwise reactive metal complexes to find more stable alternative structures. For example, all attempts to prepare reactive metallasilsesquioxanes containing bare trivalent transition-metal or heavier main-group atoms (e.g., **9** with M = Ti,[4a] V,[4b] Al,[3a] Ga,[14a] Y[14b]) have afforded dimers with siloxy-bridged structure **10**.

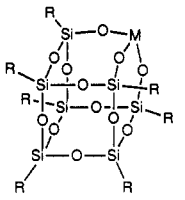

9

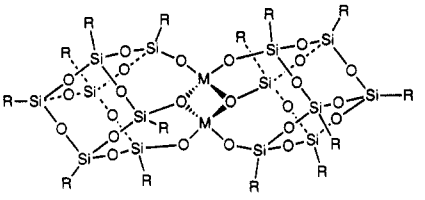

10

Structure **9** is also not favorable for boron because a single silsesquioxane framework derived from **1** is unable to support the trigonal planar BO_3 arrangement required to maximize π-bonding between oxygen and boron. If the boron atom in **9** is considered to be sp^3-hybridized, then the vacant hybrid orbital would be directed away from the oxygen atoms and unavailable for π-bonding to oxygen. Alternatively, if boron uses only p-orbitals in its σ-bonding interactions with oxygen, then the remaining s-orbital does not have the proper symmetry to engage in π-bonding with the lone pair orbitals on oxygen. Rather than adopting the siloxy-bridged structure **10**, boron satisfies its bonding requirements through a nonbridged dimeric structure with trigonal planar BO_3 moieties.

The work described here has two important implications for the chemistry of metallasilsesquioxanes. First, it demonstrates that trigonal planar coordination environments can be supported by trisilanol **1** through dimeric structures such as **2**. Second, it

(14) (a) Feher, F. J.; Budzichowski, T. A.; Ziller, J. W. Manuscript in preparation. (b) Feher, F. J.; Newman, D. A. Unpublished results.

demonstrates that seemingly major conformational changes involving silsesquioxane frameworks can occur with very low activation barriers ($\Delta H^{\ddagger} < 10$ kcal/mol).

Acknowledgment. These studies were supported by the National Science Foundation (CHE-9011593) and an NSF-Presidential Young Investigator Award (CHE-8657262). Acknowledgment is also made to the donors of the Petroleum Research Fund, administered by the American Chemical Society, for partial support of this research. Funds for the purchase of the X-ray diffraction equipment were made available from NSF Grant CHE-85-14495. F.J.F. gratefully acknowledges financial support from an Alfred P. Sloan Foundation Research Fellowship.

Supplementary Material Available: X-ray crystal data for **2**, including text detailing the experimental procedures, tables of crystal data, atomic coordinates and isotropic thermal parameters, bond lengths, bond angles, anisotropic thermal parameters, and hydrogen atom coordinates, and ORTEP drawings and a table of chemical shifts and coefficients used to simulate variable temperature ^{13}C and ^{29}Si NMR spectra (19 pages). Ordering information is given on any current masthead page.